MOLEKUL
eISSN: 2503-0310

Articles
https://doi.org/10.20884/1.jm.2026.21.1.11084

Synthesis and in Silico Studies of 1,3,5-Triaryl-2-Pyrazoline Derivatives Containing Chloro Substituent and Pyrrolidine Moiety

Jasril Jasril[1], Ihsan Ikhtiaruddin[2], Nisa Ulhukmi[1], Riryn Novianty[1], Mhd. Muslim Syaifullah[1], Neni Frimayanti[2]*

[1]Department of Chemistry, University of Riau, Pekanbaru-28293, Riau, Indonesia

[2]Department of Pharmacy, Sekolah Tinggi Ilmu Farmasi (STIFAR) Riau, Pekanbaru-28293, Riau, Indonesia

*Corresponding author email: nenifrimayanti@gmail.com

Received January 15, 2024; **Accepted** March 03, 2026; **Available online** March 20, 2026

ABSTRACT. Pyrazoline is a well-known group of five-ring heterocyclic compound containing two nitrogen atoms that has a wide range of promising biological activities. The aim of this research is to synthesize 1,3,5-triaryl-2-pyrazoline derivatives with chloro substituent and pyrrolidine moiety and to explore their potency as inhibitors for cervical cancer. The synthesis was performed through three-steps reactions. Firstly, synthesis of chlorinated naphthalenyl chalcones through Claisen-Schmidt condensation. Secondly, synthesis of chlorinated naphthalenyl pyrazolines through nucleophilic addition of phenylhydrazine to the chalcone and followed by intramolecular cyclization. Thirdly, synthesis of pyrazoline derivatives by adding the pyrrolidine moiety through O-alkylation reaction. Then, the in silico studies through molecular docking, ADME profiling, and toxicity prediction were performed to explore the potency of the synthesized compounds as inhibitors of cervical cancer by inhibiting the activity of Sirtuin-1 (SIRT-1) (PDB ID: 4I5I). The structure of all pyrazoline derivatives (**4a-4c**) were confirmed by spectroscopic analysis including UV, FT-IR, HRMS, and NMR. Based on the docking study, compound **4a** with binding free energy of -12.59 kcal/mol exhibited better potency as SIRT-1 inhibitor than previously reported inhibitor (EX527). Then, based on the ADME profiling and toxicity prediction, it can be concluded that compound **4a** exhibited reasonable drug properties with low toxicity potency (predicted LD_{50} = 1000 mg/kg).

Keywords: : Cervical cancer, molecular docking, pyrazoline-pyrrolidine, pyrazoline synthesis, sirtuin-1

INTRODUCTION

Pyrazolines exhibited several potent biological activities. For this reason, many researchers designed and synthesized these compounds and it derivatives with various structures to explore and find the structures that can be used as lead compounds in drug design. Our recent works reported that pyrazolines exhibited potent *in vivo* anti-inflammatory activity (Jasril et al., 2019), *in vivo* antidiabetic activity (Ikhtiarudin et al., 2019), *in silico* and *in vitro* cytotoxic activities on cervical cancer (HeLa) cell line (Jasril et al., 2020; Jasril et al., 2021).

Cervical cancer is the second highest cause of death in women (Siegel et al., 2021). Cervical cancer is related to the sirtuin protein in the human body. Sirtuins are nicotinamide adenine dinucleotide (NAD+)-bound deacetylases that deacetylate histones, the tumor suppressor protein p53 and several other transcription factors. It has been reported that SIRT1 promotes the growth and cisplatin resistance of carcinoma cells. Therefore, sirtuin receptor 1 (SIRT1) is used as a target for cervical anticancer treatment because SIRT1 inhibitors show increased sensitivity of 5-fluorouracil to cancer cells (Hwang et al., 2014).

Currently, cervical anticancer drugs are less selective and effective, so still cause side effects. Therefore, it is important and urgent to do a research to discover new compounds that have the ability to inhibit cancer cells better than existing compounds. Literature studies have been carried out to determine the types of substituents that can increase the pharmacophore activity of the pyrazoline ring. However, based on the results of these studies, pyrazoline compounds which are substituted for chlorophenyl and naphthalenyl rings which contain pyrrolidine groups have not been found. Therefore, in this research, synthesis of pyrazoline derivatives substituted by chlorophenyl and naphthalene rings containing pyrrolidone groups was carried out. Confirmation of the structure of the synthesized compounds was analyzed through UV, FT-IR, HRMS, and NMR spectroscopies. Modification of the structure of this pyrazoline compound is expected to be a potential candidate as an anticancer agent for breast and cervix. The synthesis target molecules were

predicted or their anticancer activity in silico through molecular docking, ADME profiling and prediction of toxicity. Binding free energy (S) and types of interactions between target molecules and SIRT1 receptors were obtained from the results of molecular docking studies.

EXPERIMENTAL SECTION

Material and Methods

The materials used in this research are 2'-hydroxy-1-acetylnaphthalene (Sigma-Aldrich), chlorinated benzaldehyde (Merck), phenyhydrazine (Merck), 1-(2-chloroethyl)pyrrolidine hydrochloride (Sigma-Aldrich), sodium hydroxide (Merck), and potassium carbonate (Merck). The organic solvents used such as ethanol absolute (Merck), and acetonitrile (Merck).

Synthesis of 1,3,5-triaryl-2-pyrazoline derivatives with chloro substituen and pyrrolidine moiety **(4a-c)** were performed in three-steps reaction. The syntesis of compounds **2a-c** were performed under microwave iradiation (Elektrolux), the synthesis of compounds **3a-c** were performed through heating in a monowave reactor (Monowave 50, Anton Paar), and the synthesis of compounds **4a-c** were performed under reflux condition, as depicted in **Figure 1**. The melting points were measured using Fischer John melting point apparatus. The HPLC chromatogram were measured using HPLC (UFLC Prominance-Shimadzu LC solution, UV SPD 20AD detector). The UV spectra were measured using spectrophotometer UV-Vis (Genesys 10S UV-Vis v44.002 2L9N175013). The FT-IR spectra were measured using spectrophotometer FT-IR (Shimadzu, IR Prestige-21). The mass spectra were measured using mass spectrometer (Water LCT premier XE, positive mode). The NMR spectra were measure using spectrometer NMR (Agilent, 500 MHz for ^{1}H NMR and 125 MHz for ^{13}C NMR).

General procedure for synthesis chlorinated naphthalenyl chalcones (2a-c)

Compound **1** (3 mmol) and various chlorinated benzaldehydes (3 mmol) were dissolved in ethanol absolute (7 mL) and sodium hydroxyde solution (3N, 4 mL) was added. The mixture was irradiated in a microwave (180 W, 5 minutes). The progress of reaction was monitored by TLC analysis. After the reaction was competed, the cold distiled water was added and the mixture was netralized by adding hydrochloric acid solution (3N) to afford the precipitate. The mixture of product was cooled for 24 hours in a refrigerator and the precipitate was filtered and washed using cold distilled water and cold n-hexane by vacuum filtration. The crude product was recrystalized in hot ethanol to obtain the pure product **2a-c**.

General procedure for synthesis chlorinated naphthalenyl pyrazolines (3a-c)

Compound **2a-c** (1 mmol) and phenylhydrazine (1.5 mmol) were dissolved in ethanol absolute (7 mL) and sodium hydroxyde solution (3N, 2 mL) was added. The mixture was heated in a monowave reactor (80 °C, 1 hour). The progress of reaction was monitored by TLC analysis. After the reaction was competed, the cold distiled water was added and the mixture was netralized by adding hydrochloric acid solution (3N) to afford the precipitate. The mixture of product was cooled for 24 hours in a refrigerator and the precipitate was filtered and washed using cold *n*-hexane and methanol by vacuum filtration. The crude product was recrystalized in hot ethanol to obtain the pure product of **3a-c**.

General procedure for synthesis pyrazoline derivatives with chloro substituent and pyrrolidine moiety (4a-c)

Compound **3a-c** (1 mmol) and 1-(2-chloroethyl)pyrrolidine hydrochloride (1.5 mmol) were dissolved in acetonitrile (5 mL) and potassium carbonate powder (1.5 mmol) was added. The mixture was refluxed (70-75 °C, 6 hours). The progress of reaction was monitored by TLC analysis. After the reaction was competed, the solvent was evaporated using vacuum rotary evaporator and the cold saturated sodium chloride solution was added to the mixture of product. The crude product was extracted using ethyl acetate (3 x 15 mL). The organic layer was

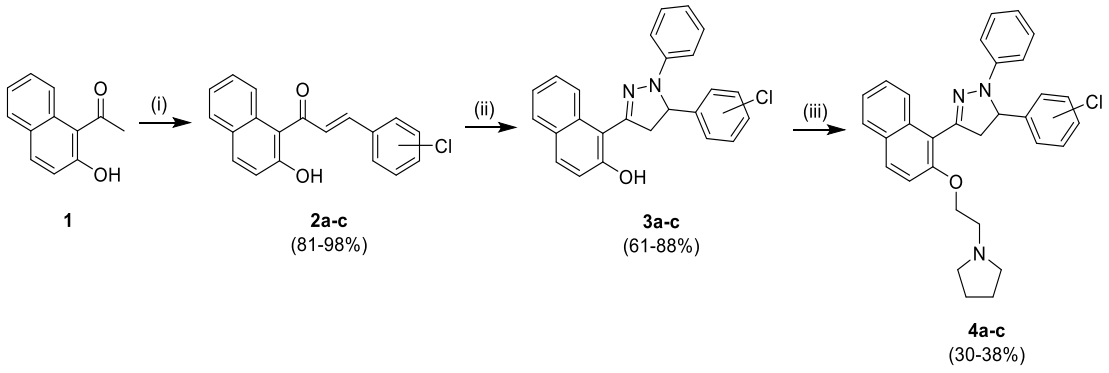

Figure 1. Synthesis route of chlorinated naphthalenyl pyrazoline derivative containing pyrrolidine moiety. Material used and reaction conditions: (i) Cl-Ph-CHO, NaOH, EtOH, 180 W MW irradiation for 5 minutes, (ii) Ph-NH-NH_2, NaOH. EtOH, monowave heating 80°C for 1 hour, (iii) 1-(2-chloroethyl)pyrrolidine, ACN, K_2CO_3, reflux 70°C for 6 hours. a = Cl in ortho position, b = Cl in meta position, c = Cl in para position.

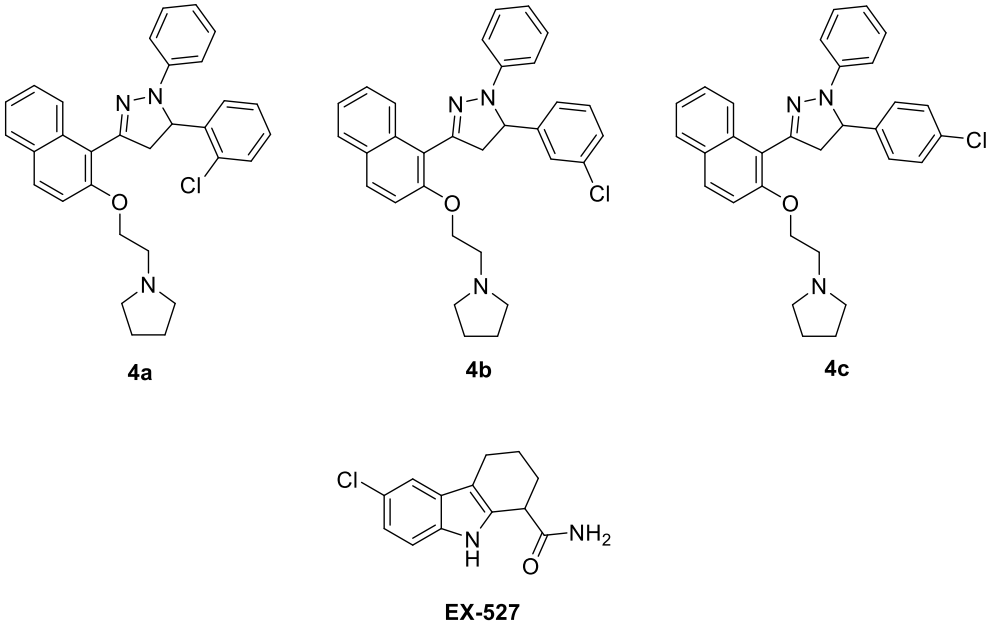

Figure 2. The 2D structure of three docked ligands (4a-c) and native ligand (EX-527)

separated, collected, and dried from water using anhydrous sodium sulphate. The organic solvent was evaporated using vacuum rotary evaporator to obtaine the crude product. The crude product was recrystalized in ethanol to obtain the pure product of **4a-c**.

Molecular Docking Study

Ligands consisted of three of these compounds (**4a-c)** and positive control (i.e. EX-527) were sketched using Chemdraw 16.0 (Cambridge Soft). furthermore, all the ligands as depicted in **Figure 2** were prepared with added Gasteiger charge, hydrogen atoms and energy minimization.

Protein was retrieved from protein databank (www.rcsb.org; PDB ID 4I5I). Water molecules was removed from the protein crystal structure followed with adding the Kollman charge, protonation and revision for the missing atoms. These steps has been done using autodock tools.

For docking computations, AutoDock Vina software's input files were created using the Lamarckian evolutionary process (Trott, et al., 2009). Docking was performed with set up parameter of number of GA runs and maximum number of evals of 100 and 5000000, respectively. The docking grid box, which covered the binding region inhabited by the co-crystallized ligand, was centered at coordinates (x, y, z) and had dimensions of 40 × 40 × 40 Å. The grid size was chosen to prevent the inclusion of unnecessary solvent regions while enabling full ligand accommodation. Docking simulation was carried out in 100 poses by displaying of 10 conformations and the best score. After docking is complete, the best conformation is selected, then exported into the receptor structure and save in pdb format. Ligand interactions with amino acid residues were visualized through the BIOVIA Discovery Studio Visualizer 2021 software.

Docking simulations produced several conformations for each of the ligands. The optimal conformation was determined by the lowest binding free energy (highest negative docking score) derived using AutoDock Vina, in conjunction with the RMSD assessment and ocular examination of ligand orientation within the active site. The chosen pose must occupy the same binding pocket as the native ligand and form advantageous interactions with adjacent amino acid residues. This conformation was used for interaction analysis and visualization.

ADME profiling

To examine the pharmacokinetics of a specific molecule that might be employed as a drug, ADME and preADMET analysis assessment are curtail. ADME predictions were carried out online through SwissADME website (http://www.swissadme.ch) dan preADMET (https://preadmet.webservice.bmdrc.org/) which provides prediction of physicochemical properties, pharmacokinetics, and drug-likeness (Daina et al., 2017)

Toxicity Prediction

Toxicity prediction is needed to examine to know the level toxicity of a new drugs. Toxicity was carried out through preADMET (https://preadmet.webservice.bmdrc.org/) and ProTox-II (http://tox.charite.de/protox_II) (Banerjee et al., 2018)

RESULTS AND DISCUSSION

Synthesis

The synthesis of pyrazoline derivatives containing chloro substitient and pyrrolidine moiety were performed through three-steps reactions, as depicted

in **Figure 1**. The first step (i) is synthesis of chlorinated naphthalenyl chalcones through Claisen-Schmidt condensation to produce compounds **2a-c**. The second step (ii) is synthesis of chlorinated naphthalenyl pyrazolines through nuchleophilic addition and followed by intramolecular cyclization to produce compounds **3a-c**.

The last step (iii) is synthesis of pyrazoline derivatives by adding the pyrrolidine moiety through O-alkylation reaction to produce compounds **4a-c**.

5-(2-chlorophenyl)-1-phenyl – 3 - (2- (2- (pyrrolidin-1-yl)ethoxy)naphthalen-1-yl)-4,5-dihydro-1H-pyrazole **(4a)**

Compound **4a** was obtained as green semi-solid in 30% yield, m.p. 110-111°C. UV spectra (EtOH), λ_{max} = 182 and 340 nm. FTIR spectra (KBr), ū (cm^{-1}) = 3056, 2904, 1499, 1270, 1061, 746. ^{1}H NMR spectra (500 MHz, CD_3OD) δ (ppm) = 8.13 (d, 1H, *J* = 8.6 Hz), 7.93 (d, 1H, *J* = 9.1 Hz), 7.84 (d, 1H, *J* = 8.2 Hz), 7.53-7.46 (m, 2H), 7.41-7.36 (m, 3H), 7.32-7.28 (m, 2H), 7.16 (t, 2H, *J* = 7.4 Hz), 6.94 (d, 2H, *J* = 7.6 Hz), 6.77 (t, 1H, *J* = 7.3 Hz), 5.71 (dd, 1H, H_x, J_{xa} = 6.6 Hz, J_{xb} = 12.1 Hz), 4.22 (t, 2H, *J* = 5.6 Hz), 3.99 (dd, 1H, H_b, J_{ba} = 17.6 Hz, J_{bx} = 12.1 Hz), 3.24 (dd, 1H, Ha, J_{ab} = 17.6 Hz, J_{ax} = 6.6 Hz), 2.76-2.65 (m, 2H), 2.54-2.50 (m, 4H), 1.71-1.66 (m, 4H). ^{13}C NMR spectra (125 MHz, CD_3OD) δ (ppm) = 154.88, 147.07, 144.95, 139.45, 132.72, 131.73, 130.65, 129.75, 129.32, 128.75, 128.63 (2C), 127.86, 127.39, 127.32, 126.85, 124.09, 123.70, 118.87, 115.71, 113.67, 112.73 (2C), 67.95, 61.08, 54.52 (2C), 54.27, 45.64, 22.75 (2C). HR-MS spectra: mass was calculated as $C_{31}H_{31}ClN_3O$ $[M+H]^+$ = 496.2156 and was found at m/z = 496.2155.

5-(3-chlorophenyl) – 1 - phenyl-3- (2-(2-(pyrrolidin-1-yl)ethoxy)naphthalen-1-yl)-4, 5-dihydro - 1H-pyrazole **(4b)**

Compound **4b** was obtained as yellow crystal in 38% yield, m.p. 115 °C. UV spectra (EtOH), λ_{max} = 280 and 338 nm. FTIR spectra (KBr), ū (cm^{-1}) = 3068, 2955, 1597, 1276, 1061, 744. ^{1}H NMR spectra (500 MHz, CD_3OD) δ (ppm) = 8.13 (d, 1H, *J* = 8.6 Hz), 7.95 (d, 1H, *J* = 9.1 Hz), 7.85 (d, 1H, *J* = 8.5 Hz), 7.49 (t, 1H, *J* = 7.7 Hz), 7.44-7.37 (m, 5H), 7.31 (td, 1H, *J* = 7.2 and 2.1 Hz), 7.16 (t, 2H, *J* = 7.3 Hz), 7.01 (d, 2H, *J* = 7.8 Hz), 6.77 (t, 1H, *J* = 7.3 Hz), 5.44 (dd, 1H, H_x, J_{xa} = 6.5 Hz, J_{xb} = 12.1 Hz), 4.26 (t, 2H, *J* = 6.2 Hz), 3.88 (dd, 1H, H_b, J_{ba} = 17.7 Hz, J_{bx} = 12.1 Hz), 3.35 (dd, 1H, H_a, J_{ab} = 17.7 Hz, J_{ax} = 6.5 Hz), 2.81-2.70 (m, 2H), 2.55-2.53 (m, 4H), 1.72-1.69 (m, 4H). ^{13}C NMR spectra (125 MHz, CD_3OD) δ (ppm) = 154.90, 146.89, 145.45, 134.53, 132.74, 130.62, 130.30, 129.33, 128.56 (2C), 127.86, 127.27, 126.83, 125.93 (2C), 124.43, 124.06, 123.68, 118.88, 115.78, 113.70, 113.02 (2C), 67.97, 63.44, 54.52, 54.20 (2C), 29.25, 22.78 (2C). HR-MS spectra: mass was calculated as $C_{31}H_{31}ClN_3O$ $[M+H]^+$ = 496.2156 and was found at m/z = 496.2155.

5-(4-chlorophenyl)- 1 - phenyl – 3 - (2-(2-(pyrrolidin-1-yl)ethoxy)naphthalen-1-yl)-4,5-dihydro-1H-pyrazole **(4c)**

Compound **4c** was obtained as light yellow crystal in 36% yield, m.p. 111-112 °C. UV spectra (EtOH), λ_{max} = 281 and 339 nm. FTIR spectra (KBr), ū (cm^{-1}) = 3056, 2956, 1597, 1270, 1061, 746. ^{1}H NMR spectra (500 MHz, CD_3OD) δ (ppm) = 8.14 (d, 1H, *J* = 8.6 Hz), 7.94 (d, 1H, *J* = 9.1 Hz), 7.85 (d, 1H, *J* = 8.0 Hz), 7.49 (t, 1H, *J* = 7.8 Hz), 7.43-7.37 (m, 6H), 7.15 (t, 2H, *J* = 7.2 Hz), 7.00 (d, 2H, *J* = 7.7 Hz), 6.76 (t, 1H, *J* = 7.4 Hz), 5.43 (dd, 1H, H_x, J_{xa} = 6.4 Hz, J_{xb} = 12.1 Hz), 4.23 (t, 2H, *J* = 5.9 Hz), 3.86 (dd, 1H, H_b, J_{ba} = 17.6 Hz, J_{bx} = 12.1 Hz), 3.30 (dd, 1H, H_a, J_{ab} = 17.6 Hz, J_{ax} = 6.4 Hz), 2.76-2.66 (m, 2H), 2.55-2.48 (m, 4H); 1.73-1.67 (m, 4H). ^{13}C NMR spectra (125 MHz, CD_3OD) δ (ppm) = 158.82, 150.75, 149.06, 145.65, 136.67, 134.55, 133.26, 132.71 (2C), 132.47 (2C), 131.80, 131.57 (2C), 130.79, 128.04, 127.63, 122.73 (2C), 119.74, 117.62, 116.94 (2C), 71.87, 67.20, 58.50, 58.15 (2C), 26.70 (3C). HR-MS spectra: mass was calculated as $C_{31}H_{31}ClN_3O$ $[M+H]^+$ = 496.2156 and was found at m/z = 496.2151.

In Silico Studies

The docking result, ADME profile, and toxicity prediction for synthesized compounds compared with reference inhibitor were presented in **Table 1**, **2**, and **3**, respectively.

Synthesis

In this work, we are succesfully synthesized three new 1,3,5-triaryl-2-pyrazoline derivatives (**4a-c**) containing chloro substituent and pyrrolidine moiety through three-steps reactions. In the first step, we synthesized chlorinated napthalenyl chalcones via Claisent-Schimdt condensation of 2′-hydroxy-1-acetylnaphthalene and benzaldehyde derivatives with chloro substituent in various positions. This reaction takes places in alkaline condition under microwave irradiation. The irradiation power of 180 W was applied in this work based on our previous study that reported that it is the most optimal irradiation power for synthesis 2′-hydroxychalcone with chloro substituent. Based on previously work, the application of irradiation power lower than 180 W will make it difficult for the intermediate (β-hydroxydihydrochalcone) to undergo dehydration to form the desired product, while application of irradiation power higher than 180 W will cause the formation of flavanone due to cyclization between hydroxyl group and β carbon under alkaline condition and it also increase the possibility of formation of the other side products that have not yet been identified (Zamri et al., 2019). The using of this iradiation power of 180 W was also reported in many literatures for synthesis chalcone analogues (Jasril *et al.*, 2019; Ikhtiarudin *et al.*, 2020). The reaction begins with the formation of enolate ion and attacking of carbonyl

carbon of benzaldehyde by enolate anion to produce β-hydroxydihydrochalcone as an intermediate via C-C bond formation, then followed by dehydration to form unsaturated α,β-ketone (chalcone) (Chang, 2015). Based on the synthesis result, we obtained pure compounds 2a, 2b, and 2c with chloro substituent in various positions (ortho, meta, and para) in a good yield, 81, 81, and 98% yields, respectively.

In the second step, we synthesized chlorinated naphthalenyl pyrazoline via nucleophilic addition of phenylhydrazine to carbonyl group of compunds **2a-c**. This reaction also takes place in alkaline condition. In this work, we tried to apply the heating method in a sealed-vessel reactor, monowave 50. Using this reactor enables to mimick the heating rates of a microwave reactor in the applicable operation volume. This reactor enables synthesis multiple times faster than traditional stirrer hot-plate setups (Zamri et al., 2019). The reaction begins with the formation of phenylhydrazine anion in alkaline solution, then the anion attacks the carbonyl group of chalcone via nucleophilic addition and then followed by intramolecular cyclization between NH and C_β to form a pyrazoline ring (Kaka *et al.*, 2019). Based on the synthesis result, we obtained pure compound **3a**, **3b**, and **3c** in 74, 88, and 61% yields, respectively.

In the third step, we synthesized the pyrazoline derivative with pyrrolidine moiety via O-alkylation. This reaction is similar with Wiliamson ether synthesis. The first step is the formation of alkoxy or aryloxy anion as a result of the reaction between the hydroxy group of pyrazoline 3a-c compounds with a solution of potassium carbonate in acetonitrile. In the second step, the aryloxy anion formed acts as a nucleophile and attacks the electrophilic carbon of the alkyl halide to form an ether group (Frimayanti et al., 2023; Frimayanti et al., 2023). This reaction is also called as a nucleophilic substitution 2 (SN_2) in which the replacement of the Cl group by the nucleophile occurs in one step (Ikhtiarudin et al., 2022). We chose the reflux method because this method has been widely reported to be successful in carrying out this reaction. Based on the synthesis result, we obtained pure compound **4a**, **4b**, and **4c** in 30, 38, and 36% yields, respectively.

The purity of the pyrazoline derivatives **4a-c** were confirmed by HPLC analysis and the structures of obtained compound were confirmed by spectroscopic analyses including UV, FT-IR, ^{1}H NMR, ^{13}C NMR, and HR-MS. The ^{1}H NMR spectra of compounds **4a**, **4b**, and **4c** showed some charactheristic signals in the aliphatic proton and carbon regions, as described in the previous report (Zamri *et al.*, 2019). These signals are generated by aliphatic protons with the ABX system which is characteristic of the protons present in the heterocyclic ring of pyrazoline. In this case, the signals of the protons H_a, H_b, and H_x appear on the chemical shift range (ppm) of 3.24-3.35 (H_a), 3.86-3.99 (H_b), and 5.43-5.71 (H_x), respectively. Protons Ha and Hb showed geminal coupling (J = 17.6-17.7 Hz), while protons Ha and Hx or Hb and Hx showed vicinal coupling as presented in result part. Based on the spectral data, we observed that the signal of proton H_x in compound **4a** (5.71 ppm) shifted toward to higher chemical shift than the signals of protons H_x in compounds **4b** and **4c** (5.43 and 5.44 ppm, respectively). This is due to the influence of the negative induction effect of the Cl substituent in the ortho position, thus causing the proton H_x in compound 4a become more unshielded.

The presence of aliphatic protons of the pyrrolidine heterocyclic ring in compounds **4a**, **4b**, and **4c** are indicated by two multiplet signals of two type of methylene groups, (CH_2-$\underline{CH_2}$)$_2$-N-] and ($\underline{CH_2}$-CH_2)$_2$-N-. The first type is methylene group bonded to the nitrogen atom. The signals of this type of methylene groups were observed at the higher chemical shift due to inductive effect form nitrogen at chemical shift range (ppm) of 2.54-2.50 (m, 4H), 2.55-2.53 (m, 4H), and 2.55-2.48 (m, 4H) in the ^{1}H NMR spectra of compounds **4a**, **4b**, and **4c**, respectively. The second type is methylene group which is not direcly attacked to nitrogen atom. The signals of this type of methylene groups were observed at the lower chemical shift (ppm) at the range of 1.71-1.66 (m, 4H), 1.72-1.69 (m, 4H), and 1.73-1.67 (m, 4H) in the ^{1}H NMR spectra of compounds **4a**, **4b**, and **4c**, respectively. In addition, two other signals in aliphatic proton area at chemical shift of 4.26-4.23 (t, 2H) and 2.81-2.65 (m, 2H) were assigned as signal of methylene group bonded to oxygen atom (-N-CH_2-**CH_2**-O-)[19] and methylene group bonded to nitrogen atom (-N-**CH_2**-CH_2-O-), respectively. These two methylene groups connected the pyrrolidone moiety to the naphthalene ring in the structure of compound **4a-c**.

The ^{1}H NMR spectra of compound **4a-c** showed the fifteen aliphatic protons which corresponds to the number of aliphatic protons in the structure of the pyrazoline derivatives **4a-c**. In addition, the spectra also showed the presence of fifteen aromatic protons which corresponds to the number of aromatic protons in their respective structures. Overall, there are 30 protons in the structure of the compounds obtained, where this number corresponds to the total protons in the pyrazoline derivatives **4a-c**. The ^{13}C NMR spectra also showed this agreement, where there are eight carbon signals in the aliphatic region and as many as twenty two carbons appear in the aromatic carbon chemical shift region which are signals from aromatic carbon in the naphthalene, phenyl and chlorophenyl rings, where a characteristic carbon signal in the chemical shift range of 158.52-154.88 ppm is a signal from the oxy-aryl carbon in the aromatic ring of naphthalenyl. In addition, there is a hydrozone carbon (C=N) signal that appears in the chemical shift range of 150.75-146.89 ppm which strengthens the conclusion of the presence of a pyrazoline ring. Then, based on the mass spectra, all the mass of the

obtained compounds also showed conformity with the mass of the expected structure with difference in mass of 0.0001-0.0005. This mass difference still meets the requirements for molecular weight measurements below 1000, the mass difference is not more than 0.0030 [16]. Overall, the results of the spectroscopic analyses of the synthesised compounds indicated conformity with the structure of the targeted compounds.

In Silico Studies

Molecular docking has been successfully carried out on synthesized compounds **4a-c** which act as ligands. Based on docking results in **Table 1**, it is seemed that compound **4a** has lower binding free energy value of -12.59 kcal/mol than native ligand EX527. The affinity of the ligand compounds for the receptor can be seen from the value of the binding free energy from the obtained docking results. The docking-derived binding energy signifies a forecasted binding affinity and reflects the probability of ligand–protein interaction according to the utilized scoring model, rather than the true thermodynamic stability of the complex. The result of a negative energy value indicated that the ligand binds to the receptor spontaneously. The more negative and smaller the docking score indicated that the conformation formed between the ligand and the receptor is more tends to form a ligand-receptor bond (Kalyaanamoorthy & Chen, 2011). In addition, The docking binding energy serves as a computer scoring function that assesses the relative probability of ligand–protein interactions, mostly utilized for the comparative ranking of compounds rather than as a direct indicator of thermodynamic stability.

Another parameter that can be used for predicting the docking results is RMSD value (Frimayanti et al 2020). It is described the suitability of the position of the tested ligand with the native ligand. Native ligands are used to determine the docking parameters to be used in the test ligands. So that the greater the RMSD value, it means that the difference in the position of the tested ligand with the native ligand when it binds to the receptor is increasingly different. Conversely, the smaller the RMSD value indicates that the tested.

Native compound was explored to interact with amino acids through van der Waals interaction and hydrophobic. This compound was able to construct hydrogen bond with Val412, His363 with binding free energy of -7.75 kcal/mol. Compound **4a** was observed to interact with amino acid residues Phe413, His363, Ile279, Asn346, Gln345, Gly261, Ser441, Arg274, Tyr280 through van der Walls interaction and hydrophobic interactions were also assumed between compound **4a** with amino acid residues Phe297, Val412, Phe273, Ile411, Ile347, Ile316, Ala262, Val445, Phe414. Additionally, root-mean-square deviation (RMSD), which should ideally be less than 2 (Frimayanti et al., 2023). In AutoDock Vina, the RMSD value signifies the deviation between various docked poses in relation to the highest-ranked pose and is mostly utilized to assess pose similarity rather than to forecast biological activity. Consequently, the evaluation of ligand potential was predominantly founded on docking score, binding orientation, and interaction analysis inside the active site. Hence this compound can be considered as potential inhibitör for cervixal cancer. Spatial arrangement of compound **4a** and native ligand in the active site are depicted in **Figure 3**.

This outcome may signify a possible constraint of the proposed chemical and implies that its efficacy should be regarded with caution. Nonetheless, the molecule continues to exhibit advantageous anticipated interactions inside the active site, suggesting it may function as a viable lead structure for future optimization rather than a definitive therapeutic candidate.

The expected binding conformations were compared with the experimentally derived structure associated with the identical PDB entry. The docked ligands occupied the identical active-site region as the co-crystallized ligand and engaged with many critical residues identified in the crystallographic analysis. This substantiates the reliability of the docking results

Superimpose was used to examine simultaneously the orientation of ligands (i.e. compound **4a** and native ligand). it appears that both of these compounds have the same orientation to connect with the protein. Overlay of compound **4a** and native ligand is presented in **Figure 4**.

Absorption, Distribution, Metabolism and Excretion (ADME) is one of the crucial steps to optimize the screening and testing of drug candidate thereby reducing the risk of late stages in drug development. This study was conducted to predict the properties of drug likeness molecules based on "Lipinski's rule of five", the percentage of human intestinal absorption (HIA), the percentage ability to cross the blood-brain-barrier (BBB), the percentage of plasma protein binding (PPB), and the inhibitory potential cytochrome P450, as presented in **Table 2**.

Calculation of Lipinski's rule of five was performed to determine the level of absorption or permeability of potential compounds to cross the lipid bilayer in the human body. A compound can be predicted to have good bioavailability if it follows the Lipinski rule (maximum MW 500, log P not greater than 5, hydrogen bond donors less than 5, and hydrogen bond acceptors less than 10). Based on ADME calculations, compounds 4a, 4b, and 4c followed the drug candidate standards based on the Lipinski rule. However, the log P value of each of these compounds was still above 5, namely 6.05, 5.98, and 6.01 respectively. Log P is a partition coefficient that affects drug transfer in the pharmacokinetic phase (drug solubility in water/fat) thus it can be used to determine where the drug works (Nogrady & Donal, 2005). If the log P value is too low, the compound will be too

soluble in water but it cannot pass through the lipid barrier. Conversely, if the log P value is too high, the compound will dissolve in fat and sometimes cannot reach the target.

Table 1. Docking result of compounds 4a-c to SIRT-1

Compounds	RMSD	Binding Free Energy (kal/mol)	Interactions with SIRT-1			Binding factor*
			H bond	van der Waals	Hydrophobic	
4a	0.00	-12.59	-	Phe413, His363, Ile279, Asn346, Gln345, Gly261, Ser441, Arg274, Tyr280	Phe297 Val412, Phe273, Ile411, Ile347, Ile316, Ala262, Val445, Phe414	10
4b	0.00	-12.40	-	Arg274, Phe413, Pro271, Ile279, Asn346, His363, Gln345, Gly261, Ser441	Phe297, Phe273, Val412, Val445, Phe414, Ile270, Ile316, Ile347, Ile411, Ala262	11
4c	0.00	-12.50	-	Phe413, Asn346, Asp348, Gln345, Arg274, Gly261, Ser265, Pro271, Asp272, His363, Val412	Ile411, Ile347, Ala262, Phe297, Ile270, Ile316, Phe273	6
EX527	0.00	-7.75	Val412, His363	Val445, Arg274, Leu443, Ser441, Ser442, Gly261, Gln345, Asn346, Ile411, Ile347, Phe297	Phe273, Ala262	-

*Binding factors characterized as amino acids, their potential as inhibitors is further corroborated by their robust binding affinity, which demonstrates an overlap in the binding site residues with the positive control.

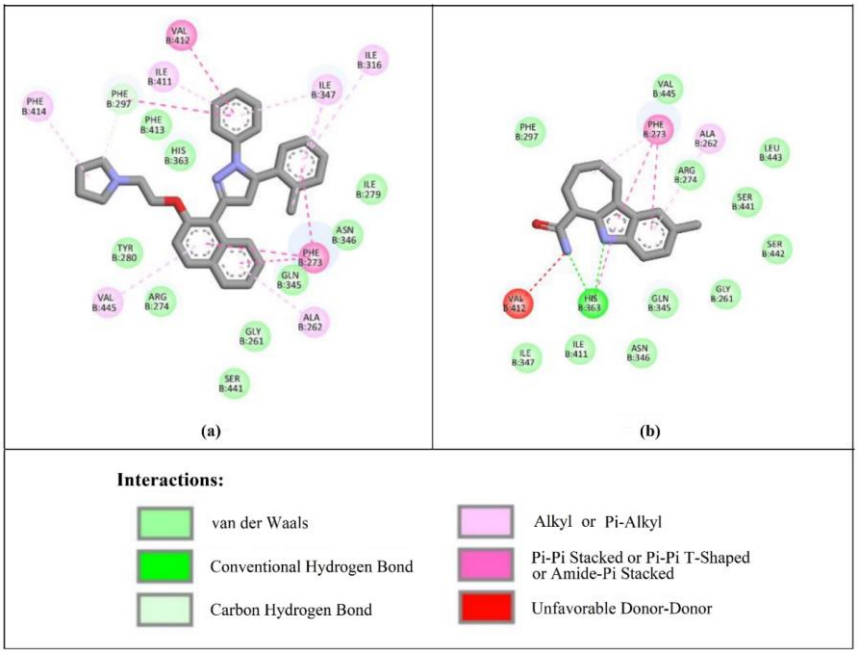

Figure 3. Visualization of interactions of (a) compound 4a and (b) EX527 as native ligand in the active site of SIRT-1

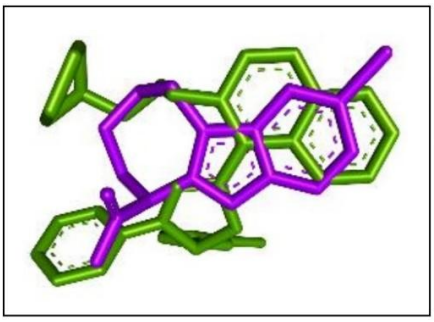

Figure 4. Overlay of binding poses of synthesized compounds **4a** (green) and the native ligand EX527 (purple) in the active site of SIRT-1.

Table 2. Result of ADME profiling of compounds **4a-c**

Profiles	4a	4b	4c	EX527
MW [a]	496.04	496.04	496.04	248.71
Log concentration ($P_{o/w}$) [a]	6.05	5.98	6.01	2.43
Num. H-bond donors [a]	0	0	0	2
Num. H-bond acceptors [a]	3	3	3	1
Rotable bonds [a]	7	7	7	1
Druglikeness (Lipinski) [a]	Yes	Yes	Yes	yes
Water solubility (mg/mL) [a]	7.51e-5 (low soluble)	7.51e-6 (low soluble)	7.51e-6 (low soluble)	1.06e-1 (high soluble)
Bioavailability score [a]	0.55	0.55	0.55	0.55
HIA (%) [b]	100.000000	100.000000	100.000000	100.000000
Caco2 (nm/sec)[2] [b]	57.0254	56.9228	56.9374	21.3007
MDCK (nm/sec)[2] [b]				
PBB (%) [b]	84.9955	84.9287	85.8253	90.9490
BBB (%) [b]	2.2391	2.0707	2.0314	4.1036
CYP1A2 inhibitor [a]	No	No	No	yes
CYP2C19 inhibitor [a]	No	No	No	yes
CYP2C9 inhibitor [a]	Yes	Yes	Yes	no
CYP2D6 [a]	Yes	Yes	Yes	yes
CYP3A4 [a]	Yes	Yes	Yes	no

Table 3. Result of toxicity prediction of compounds **4a-c**

Toxicity	4a	4b	4c	EX527
Mutagenesis (Ames Test) [a]	Mutagen	Mutagen	Mutagen	Mutagen
Mutagenesis [b]	-	-	-	-
Carcinogenicity (mice) [a]	-	-	-	+
Carcinogenicity (mouse) [a]	-	-	-	-
Carcinogenicity [b]	-	-	-	-
Immunotoxicity [b]	+	+	+	-
Cytotoxicity [b]	-	-	-	-
Cardiotoxicity [a]	Low	Low	Low	middle
Hepatotoxicity [b]	-	-	-	-
Acute toxicity LD_{50} (mg/kgBW) [b]	1000	1000	1000	705

[a] predicted using preADMET server
[b] predicted using ProTox-II server

Permeability of the three compounds in the human intestine and their distribution across the BBB were also calculated. HIA data is the sum of bioavailability and absorption assessed by excretion ratio or cumulative excretion in urine, bile and feces. BBB is presented as a ratio of concentration in the brain and blood. ADME calculations show that these three compounds are well absorbed in the human intestine and their high ability to cross the BBB indicated that these compounds are CNS active compounds. The high BBB percent values of the three compounds (**4a-c**) can prove that the compounds can still penetrate the lipid barrier strongly even though the log P value is slightly more than 5. Then, the calculation of PPB levels shows that the three compounds are not strongly bound to plasma proteins. This is different from the native compound EX527 which are strongly bound to plasma proteins. Plasma protein binding refers to the degree which a drug is bound to proteins in the blood because only drugs that are not tightly bound are efficient at diffusing or crossing cell membranes to reach their targets and provide pharmacological activity (Shargel, 2005).

Metabolism is one of the important profiles that needs to be studied. The drug will be metabolized in the liver and this process is assisted by several isozymes such as cytochrome P450. These isozymes are responsible for the biotransformation and metabolism of various drugs. Metabolism through the cytochrome P450 system has emerged as an important determinant in the occurrence of many drug interactions that can result in drug toxicity, reduced pharmacological effects, and adverse drug reactions. Therefore, it is important to recognize what the drug is involved as substrates, inducers, or inhibitors of cytochrome P450. Cytochrome P450 protein (CYP450) is a superfamily of metabolizing enzymes in the liver and is one of the biomarker proteins to determine the effect of anticancer drug responses. Inhibition of this isoenzyme is certainly one of the main causes of drug-drug interactions related to pharmacokinetics leading to toxic or other unwanted side effects due to lower clearance and accumulation of drugs (its metabolites) [21]. Therefore, new drug discovery is important for predicting the predisposition of molecules that will cause significant drug interactions through CYP inhibition, as well as for determining which isoforms are affected. Based on ADME calculations using SwissADME, the three compounds (**4a-c**) showed the potential to inhibit CYP2C9, CYP2D6, and CYP3A4. However, these compounds do not have the potential to inhibit CYP1A2 and CYP2C19. Overall, the ADME profile of the three compounds still shows reasonable medicinal properties.

In silico toxicity prediction using ProTox-II showed that the three test compounds and the two control compounds were not mutagenic (negative result), as presented in Table 3. Based on preADMET predictions, three of these compounds (4a-c) were shown negative results for predicting carcinogenicity whether in mice and also in mouse. Only compound EX527 showed positive results in predicting carcinogenicity in mice, but this compound showed negative carcinogenicity prediction. Predictions using ProTox-II also showed that compounds **4a, 4b** and **4c** are immunotoxic to human cells. The prediction of hERG inhibition using preADMET showed that compounds **4a, 4b,** and **4c** had a low risk of cardiotoxicity, but compound EX527 has moderate risk. Then, to ensure the safety of the use of the three compounds. Compounds **4a**, **4b**, and **4c** can be predicted to have lower toxicity potential than compound EX527 as a reference.

CONCLUSIONS

Three chlorinated naphthalenyl pyrazoline derivative containing pyrrolidine moiety (**4a**, **4b**, and **4c**) were succesfully synthesized through three-steps reaction. Compound **4a** with chloro substituent in ortho position exhibited the best potency as SIRT-1 inhiibitor. ADME profiling and toxicity prediction of compound **4a** also showed reasonable drug properties with low toxicity potency. Hence, compound **4a** was then chosen as the reference for the next stage in the drug design.

ACKNOWLEDGEMENTS

Thank DIPA Universitas Riau for financial support through *Program Penelitian Skema Unggulan* 2023 with contract No. 8351/UN19.5.1.3/AL.04/2023. This article is especially dedicated in memory of our dear collogue, Prof. Dr. Adel Zamri, MS, DEA.

REFERENCES

Chang K. (2015). MSc Thesis. The complete mechanism or chalcone formation. Department of Chemistry, University of California, San Diego, California, United State, https://escholarship.org/uc/item/0t65x4dd

Daina, A., Oliver, M., Vincent, Z. (2017) SwissADME: a free web tool to evaluate pharmacokinetics, drug-likeness and medical chemistry friendliness of small molecules. *Scientific Reports*. 7(4), 1-13. DOIhttps://doi.org/10.1038/srep42717

Frimayanti, N., Ikhtiarudin, I., Septama, A.W., Susanty, A., Isroq, N.D. (2023). Synthesis, in silico and structural insight of flavonol derivative compounds as new competitive dengue NS2B/NS3 protease inhibitor. *Journal of Research in Pharmacy*. 27(3): 1157-1169. http://dx.doi.org/10.29228/jrp.406

Frimayanti, N, Yaeghoobi, M., Namavar, H., Ikhtiarudin, I., Afzali, M. (2020). In silico studies and biological evaluationn of chalcone-based 1,5-benzothiazepines as new potential H1N1 neuraminidase inhibitors. *Journal of Applied*

Pharmaceutical Science, 10(10):086–094. DOI: 10.7324/JAPS.2020. 1010010

Frimayanti, N., Ikhtiarudin, I., Dona, R., Putri, I., Septama, A. W. (20230. Synthesis of 3'-methoxy flavonol and its derivatives as potential inhibitors for Dengue NS2B/NS3 and molecular insight into binding interaction. *Pharmacy Education.* 23(2): 231-243. https://doi.org/10. 46542/pe.2023.232.231243

Frimayanti, N., Ikhtiarudin, I., Septama, A.W., Susanty, A., Isroq, N. D. (2023). Synthesis, In Silico and Structural Insight of Flavonol Derivative Compounds as New Competitive Dengue NS2B/NS3 Protease Inhibitor. *Journal of Research in Pharmacy*. 27(3): 1157-1169. http://dx.doi.org/10.29228/jrp.406

Hwang, B. J., Madabushi, A., Jin, J., Lin, S.Y., Lu, A. L. (2014). Histone/protein deacetylase SIRT1 is an anticancer therapeutic target. *American Journal of Cancer Research*. 4(3):211-21.

Ikhtiarudin, I., Agistia, N., Frimayanti, N., Harlianti, T., Jasril. (2020). Microwave-assisted synthesis of 1-(4-hydroxyphenyl)-3-(4-methoxyphenyl)prop-2-en-1-one and its activities as an antioxidant, sunscreen, and antibacterial. *Jurnal Kimia Sains dan Aplikasi.* 23(2): 51-60. https://doi.org/ 10.14710/jksa.23.2.51-60

Ikhtiarudin, I., Dona, R., Frimayanti, N., Utami, R., Susianti, N., Septama, A.W. (2022). Sintesis, karakterisasi struktur, dan kajian molecular docking senyawa turunan 4'-metoksi flavonol sebagai antagonis estrogen reseptor alpha (ER-α) pada kanker payudara. *Jurnal Riset Kimia.* 13(2): 236-248. https://doi.org/10.25077/ jrk.v13i2.553

Ikhtiarudin, I., Frimayanti, N., Jasril. (2019). Microwave-assisted synthesis and in vivo anti-diabetic activity of 5-(2-bromophenyl)-3-(naphthalen-1-yl)-4,5-dihydro-1*H*-pyrazole. In: Rahmayati & Taylor (Eds). Impowering Science and Mathematics for Global Competitiveness. Taylor & Francis Group, London, 35-40. https://www.taylorfrancis.com/chapters/edit/1 0.1201/9780429461903-6

Jasril, J., Frimayanti, N., Ikhtiarudin, I. In: Mart *et al*. (Eds). (2020). Comunicating Basic Sciences for Suistainable Development. *AIP Conference Proceedings.* 2242(1), pp.040008. https://doi.org/10.1063/5.0009375

Jasril, J., Nurulita, Y., Deviana, L., Ikhtiarudin, I., Frimayanti, N. (2021). Microwave-assisted synthesis of a fluorinated pyrazoline, in silico study and in vitro cytotoxic evaluation against HeLa cell line. In: Meiliasari *et al*. (Eds). Transforming Research and Education of Science and Mathematics in the Digital Age. *AIP Conference Proceedings*. 2331(1), pp.040014. https://doi.org/10.1063/5.0042009

Jasril, Teruna, H. Y., Frimayanti, N., Hasti, S., Ikhtiarudin I. (2019). Design, molecular docking study, synthesis and in vivo evaluation of some bromonaphthyl pyrazolines as new anti-inflammatory agents. In: Rahmayati & Taylor (Eds). Impowering Science and Mathematics for Global Competitiveness. Taylor & Francis Group, London. 41-47. https://www.taylorfrancis.com/chapters/edit/1 0.1201/9780429461903-7

Kaka, K.N., Taher, S.G., Hamad, W. M., and Ibrahim, A. H. (2019). Synthesis of new series of pyrazoline, and study their kinetics and reaction mechanism. *ARO-The scientific journal of koya university*. 7(2): 5-13. https://doi.org/10. 14500/aro.10508

Kalyaanamoorthy, S., & Chen, Y. P. 92011). Structure-based drug design to augment hit discovery. *Drug Discovery Today*, *16*(17-18), 831–839. DOI: 10.1016/j.drudis.2011.07.006

Mora E, Teruna, H. Y., Frimayanti, N,. Ikhtiarudin, I., Herfindo, N., Zamri, A. (2023). Synthesis, molecular docking study, and in vivobiological evaluation of pyrazolopyridines derived from monocarbonyl curcumin analogues as potential anti-inflammatory agents. *Pharmacy Education*. 23(2): 200-206. https://doi.org/10. 46542/pe. 2023.232.200206

Nogrady, T & Donal F. W. *Medicinal Chemistry: A Molecular and Biochemical Approach*, 2005, Oxford University Press, New York.

Shargel, Leon. (2005). *Applied Biopharmaceutics & Pharmacokinetics 13: Pharmacogenetics and Drug Metabolis,* Medical Pub.

Siegel, R. L., Miller, K. D., Fuchs, H. E., Jemal, A. (2021). Cancer Statistics, *CA: A Cancer Journal for Clinicians.* 71(1):7-33. doi: 10.3322/caac. 21654

Trott, O., Olson, A.J. (2009). AutoDock Vina: Improving the speed and accuracy of docking with a new scoring function, efficient optimization, and multithreading. *Journal of Computational Chemistry. 31*, 455–461

Zamri, A., Teruna, H. Y., Ikhtiarudin, I. (2016). The influences of power variations on selectivity of synthesis reaction of 2'-hydroxychalcone analogue under microwave irradiation. *Molekul.* 11(2): 299-307. http://dx.doi.org/10. 20884/1.jm. 2016.11.2.220

Zamri, A., Teruna, H. Y., Wulansari, S., Herfindo, N., Frimayanti, N., Ikhtiarudin, I. 3-(3,4-Dimethoxyphenyl)-5-(2-fluorophenyl)-1-phenyl-4,5-dihydro-1*H*-pyrazole. *Molbank.* 2019, 2019(4): M1088. https://doi.org/10. 3390/M1088